

Zinc sulfide on GaP(110): Characterization of epitaxial growth and electronic structure

Cite as: Journal of Vacuum Science & Technology A **14**, 844 (1996); <https://doi.org/10.1116/1.580401>
 Submitted: 16 October 1995 • Accepted: 18 March 1996 • Published Online: 04 June 1998

D. Wolfframm, P. Bailey, D. A. Evans, et al.



View Online



Export Citation

ARTICLES YOU MAY BE INTERESTED IN

High temperature growth of ZnS and ZnMgS by molecular beam epitaxy under high sulfur beam pressure

Journal of Applied Physics **87**, 4249 (2000); <https://doi.org/10.1063/1.373061>



HIDEN
ANALYTICAL
Instruments for Advanced Science

<ul style="list-style-type: none"> ■ Knowledge, ■ Experience, ■ Expertise <div style="background-color: #800000; color: white; text-align: center; padding: 5px; margin-top: 10px;"> Click to view our product catalogue </div> <p style="font-size: 0.8em; margin-top: 10px;">Contact Hiden Analytical for further details: W www.HidenAnalytical.com E info@hiden.co.uk</p>	<div style="text-align: center;"> <p style="font-weight: bold; font-size: 0.8em;">Gas Analysis</p> <ul style="list-style-type: none"> ▶ dynamic measurement of reaction gas streams ▶ catalysis and thermal analysis ▶ molecular beam studies ▶ dissolved species probes ▶ fermentation, environmental and ecological studies </div>	<div style="text-align: center;"> <p style="font-weight: bold; font-size: 0.8em;">Surface Science</p> <ul style="list-style-type: none"> ▶ UHVTPD ▶ SIMS ▶ end point detection in ion beam etch ▶ elemental imaging - surface mapping </div>	<div style="text-align: center;"> <p style="font-weight: bold; font-size: 0.8em;">Plasma Diagnostics</p> <ul style="list-style-type: none"> ▶ plasma source characterization ▶ etch and deposition process reaction kinetic studies ▶ analysis of neutral and radical species </div>	<div style="text-align: center;"> <p style="font-weight: bold; font-size: 0.8em;">Vacuum Analysis</p> <ul style="list-style-type: none"> ▶ partial pressure measurement and control of process gases ▶ reactive sputter process control ▶ vacuum diagnostics ▶ vacuum coating process monitoring </div>
--	---	--	---	---

Zinc sulfide on GaP(110): Characterization of epitaxial growth and electronic structure

D. Wolframm

AMRL, Athrofa Gogledd Ddwyrain Cymru (NEWI), Wrexham LL 11 2 AW, United Kingdom

P. Bailey

SRS, Daresbury Laboratory, Warrington WA 4 4 AD, United Kingdom

D. A. Evans

AMRL, Athrofa Gogledd Ddwyrain Cymru (NEWI), Wrexham LL 11 2 AW, United Kingdom

G. Neuhold and K. Horn^{a)}

Fritz-Haber-Institut der Max-Planck-Gesellschaft, Faradayweg 4-6, D-14195 Berlin, Germany

(Received October 16 1995; accepted March 18 1996)

Epitaxial layers of ZnS were grown on cleaved GaP(110) surfaces by molecular beam epitaxy in an ultrahigh vacuum photoelectron spectrometer. The growth mode and the structure of the overlayer were studied by means of low-energy electron diffraction (LEED) and core as well as valence level photoemission using synchrotron radiation. The attenuation of substrate core-level intensities with ZnS deposition indicate layerwise growth. LEED demonstrates the growth of the cubic (zinc-blende) phase as expected for substrate-stabilized growth. A minor interface reaction is evident from changes in the appearance of the substrate (Ga 3*d*) and overlayer (S 2*p*) core levels with increasing thickness. S–Ga bonding was observed in a thin interfacial layer. The valence band offset for this lattice-matched heterojunction interface system was determined, and found to be of the straddling type (type I); its magnitude is in agreement with predictions based on the dielectric midgap energy model. © 1996 American Vacuum Society.

I. INTRODUCTION

Current activities concerning light-emitting semiconductor devices in the blue-green region of the spectrum have led to renewed interest in the electronic properties of II–VI compound semiconductor materials. With respect to the growth of thin films on III–V substrates, an investigation of their interface chemistry and the charge transport barriers between substrate and overlayer is important. In the recently demonstrated blue-green lasers ZnSe and its alloys with ZnS are used as cladding layers and for the creation of lattice-matched epitaxial layers to a GaAs substrate.¹ Here we report an investigation of zinc sulfide layer growth, interface chemistry, and electronic structure with regard to heterojunction band offset. Zinc sulfide is one of the materials for which few surface studies have been carried out,^{2–5} possibly due to the lack of suitable conducting samples. As for theoretical investigations, the bulk electronic structure has recently been studied within the density-functional formalism.^{6,7} The good lattice match (a mismatch of 0.7%⁸) between cubic ZnS and GaP renders the latter ideally suited as substrate material for the growth of the cubic modification of ZnS. In an earlier study of ZnS growth on Si(111),⁹ problems with sulphur passivation of the silicon surface were observed, such that crystalline order of the layers was not perfect. Such problems were not encountered in the ZnS/GaP system, and the electronic band structure of the cubic ZnS layers could be studied in angle-resolved photoemission.

Zinc sulfide, with its large band gap (3.74 eV⁸) at the upper end of the range of the II–VI semiconductors, is particularly interesting since, with the absence of pronounced spin-orbit effects on the electronic structure, a body of theoretical work already exists, which has not been matched by experimental data. This study is part of a series of photoelectron spectroscopic and low-energy electron diffraction (LEED) studies of II–VI compound semiconductor layers such as ZnTe,¹⁰ CdS,¹¹ and CdSe¹² on lattice-matched III–V semiconductor surfaces, which have been used in order to follow trends in interfacial chemical reactions and valence band offsets, and the differences in electronic structure for a material which can crystallize in the zinc-blende and cubic modifications.

II. EXPERIMENT

Experiments were carried out in two separate ultrahigh vacuum chambers with a base pressure of 8×10^{-11} mbar, each equipped with a high-resolution angle-resolving electron energy analyzer (HA 50 and HA 100 from VSW Ltd., UK), a cleavage tool, a temperature-controlled manipulator that allowed cooling and heating of the sample, molecular beam epitaxy (MBE) cells, and LEED optics for the study of overlayer crystallinity. Crystals of GaP (MCP Ltd., UK), *n* doped, with a carrier concentration of 3×10^{17} cm⁻³ were oriented and cut to be cleaved using the double wedge technique. ZnS with 99.9999 purity (Crystal GmbH, Berlin) was deposited from a water-cooled MBE cell at a temperature of 685 °C, leading to growth rates of 2 Å/min. Amounts of deposited material were measured by means of a quartz crystal

^{a)}Author to whom correspondence should be addressed; electronic mail: Horn@fhi-berlin.mpg.de

thickness monitor (Leybold Inficon), and were calibrated in terms of overlayer thicknesses on the basis of the Ga 3*d* attenuation curve. In these experiments, core-level photoelectron spectroscopy was performed on station TGM 4 at BESSY (Berliner Elektronen-Speicherring-Gesellschaft für Synchrotronstrahlung mbH), and station 6.1 at the SRS Daresbury storage ring (Daresbury, UK). In the BESSY experiments, only the Ga 3*d*, Zn 3*d*, and valence band regions were accessible; the phosphorus 2*p* and sulfur 2*p* levels were also investigated in the runs at the Daresbury synchrotron source. Overall spectral resolution was about 70–150 meV. Spectra shown were either recorded in normal emission (BESSY runs), or at 45° to the surface normal along the [110] azimuth (Daresbury). Overlayers were grown on several different substrates in order to establish the optimal growth temperature of 150 °C, characterized by a minimum amount of interface reaction as judged from the Ga 3*d*, P 2*p*, and S 2*p* core levels, and the quality of the LEED diffraction pattern.

III. RESULTS AND DISCUSSION

A. Overlayer growth and interface chemistry

Core-level photoemission provides a means of examining overlayer growth mode from the thickness dependence of the substrate core levels, and the shape of the intensity curve as a function of deposition. The core levels available for investigation in our study are the Ga 3*d* and P 2*p* levels of the substrate, and the Zn 3*d* and S 2*p* levels of the overlayer. The Zn 3*d* peak is less suitable for an analysis of chemical reactions since it has band character, being located at a binding energy of only 9.3 eV below the valence band maximum (VBM). Thus in both sets of experiments, the intensity decrease of the Ga 3*d* peak was analyzed in terms of overlayer growth mode, but only in the Daresbury runs the P 2*p* level was also recorded and analyzed.

A set of spectra of the Ga 3*d* level, recorded at a photon energy of 80 eV, is shown in Fig. 1 for increasing depositions of ZnS on a freshly cleaved GaP(110) surface. The overall Ga 3*d* peak intensity is seen to be attenuated with ZnS exposure, and is completely absent above 46 Å. The decrease in bulk peak intensity is shown in the inset of Fig. 1 and, although the growth is not completely layer by layer, the small deviation from an exponential curve indicates the absence of island formation. As for many other systems, the attenuation rate appears different below and above ≈5 Å, and this is in part due to the initial chemical mixing below this coverage compared with ZnS growth at higher thicknesses. Selected spectra corresponding to the clean surface and coverages of 0.3 and 5.8 Å are shown resolved into constituent peaks using a nonlinear least-squares fitting routine, using accepted values for fit parameters such as the spin-orbit splitting, Lorentzian broadening, and surface core-level shift.^{13,14} The clean surface is composed of two peaks corresponding to bulk and surface Ga atoms in GaP and the almost equal intensity indicates the surface sensitivity of the experimental probe. The residuum is shown beneath each fitted spectrum. During exposure to ZnS, the Ga 3*d* peak

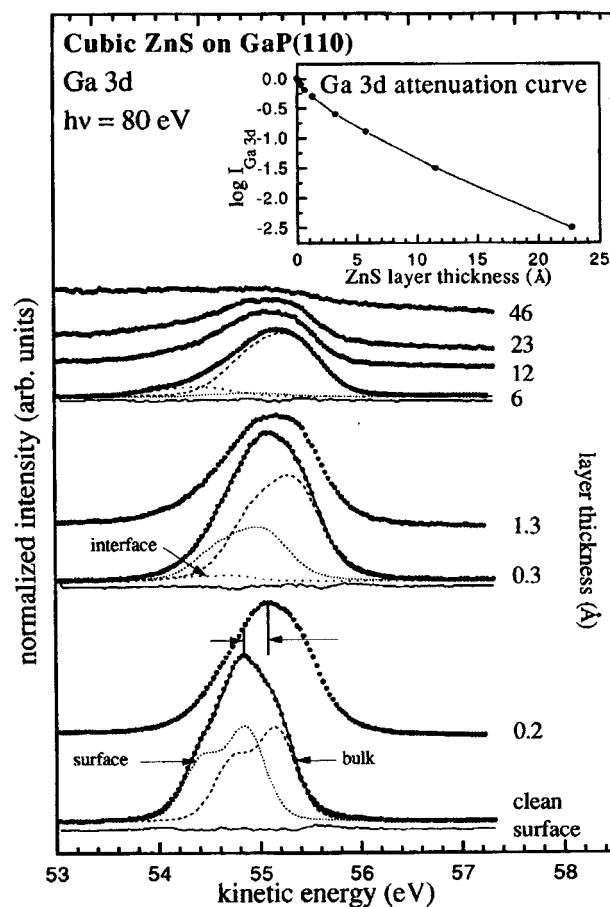


FIG. 1. Set of spectra of the gallium 3*d* peak from a GaP(110) surface exposed to doses of ZnS as indicated, recorded at a photon energy of 80 eV under an angle of emission of 45°. Inset: intensity of the gallium 3*d* peak on a logarithmic scale, as a function of ZnS layer thickness, indicating near-layerwise growth. Selected spectra are shown resolved into three components. As the ZnS grows, the surface gallium atoms are suppressed and a new low-energy component corresponding to interfacial Ga–S binding appears.

broadens and develops a shoulder at low kinetic energy (KE). At each coverage, the curve can be resolved into three peaks, with the higher kinetic energy bulk peak having the highest intensity throughout. This indicates that disruption of the bulk Ga in GaP is not large and all chemically shifted components are due to Ga atoms near the surface region. The degree of intermixing at the interface is less than reported for similar systems where extra components in the cation peak have been associated with compound formation with the group VI element. For example, in ZnTe on GaSb and ZnSe on GaAs, core-level¹⁰ and Raman scattering studies¹⁵ have indicated the formation of III₂VI₃ compounds which have the defect zinc blende structure.¹⁶ The surface peak is attenuated with increasing coverage while the lowest kinetic energy peak increases intensity relative to the bulk peak up to a coverage of 12 Å. Above this coverage, the line shape does not change further. This lower-energy peak is identified as due to Ga–S bonding, in agreement with studies of sulphur adsorption on both (111) and (001) surfaces of GaAs,^{17,18} where low-energy components at around 0.5 eV below the

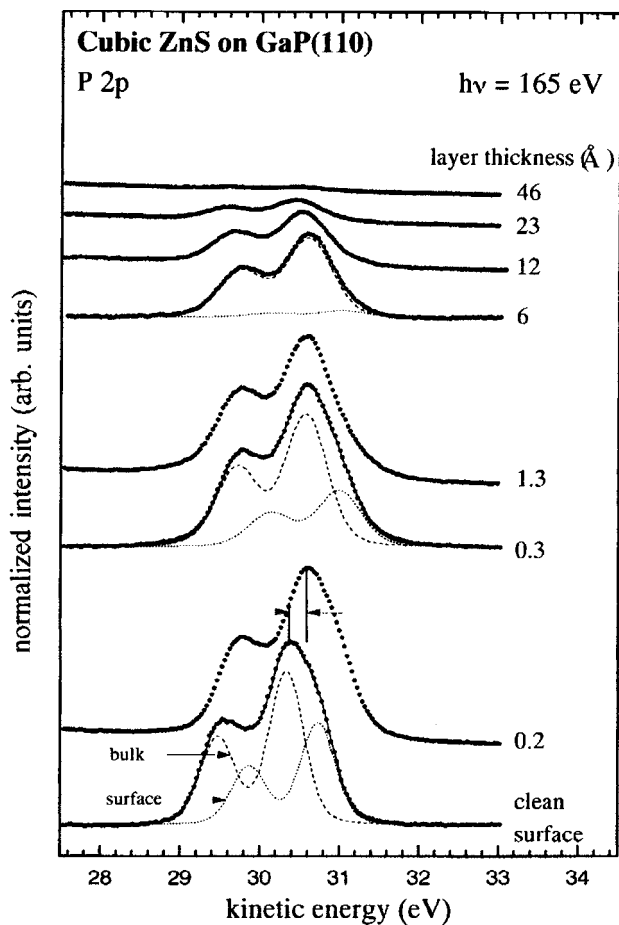


Fig. 2. Set of spectra of the phosphorus 2*p* peak for different layer thicknesses of ZnS on GaP(110) as indicated, recorded at a photon energy of 190 eV under an angle of emission of 45°. All spectra could be resolved into two spin-orbit split components corresponding to bulk- and surface-coordinated phosphorus atoms.

bulk peak were also identified as due to Ga–S bonds. It thus appears that a thin interface layer containing Ga–S bonding is present in this system.

In addition to the chemically shifted components, all peaks are seen to shift to higher kinetic energies at the first coverage of 0.2 Å, and a smaller shift to lower kinetic energy is observed above 5.8 Å. The former is due to band bending at the GaP interface due to zinc and sulfur adsorption and it is important to quantify this Fermi level shift in order to calculate the valence band offset. The smaller shift at higher coverages is also reflected in the phosphorus and sulfur core levels and is believed to be due to surface charging as the surface conductivity decreases with ZnS growth.

Corresponding emission spectra from the phosphorus 2*p* core level are shown for comparison in Fig. 2. The most striking feature in these spectra is that no extra peaks appear during ZnS growth. The surface peak at high kinetic energy is attenuated with coverage and is almost completely absent above 6 Å. This is in apparent conflict with a report by Dudzik *et al.*¹⁹ who reported a low kinetic energy component in the phosphorus 2*p* spectrum of GaP when dosed with

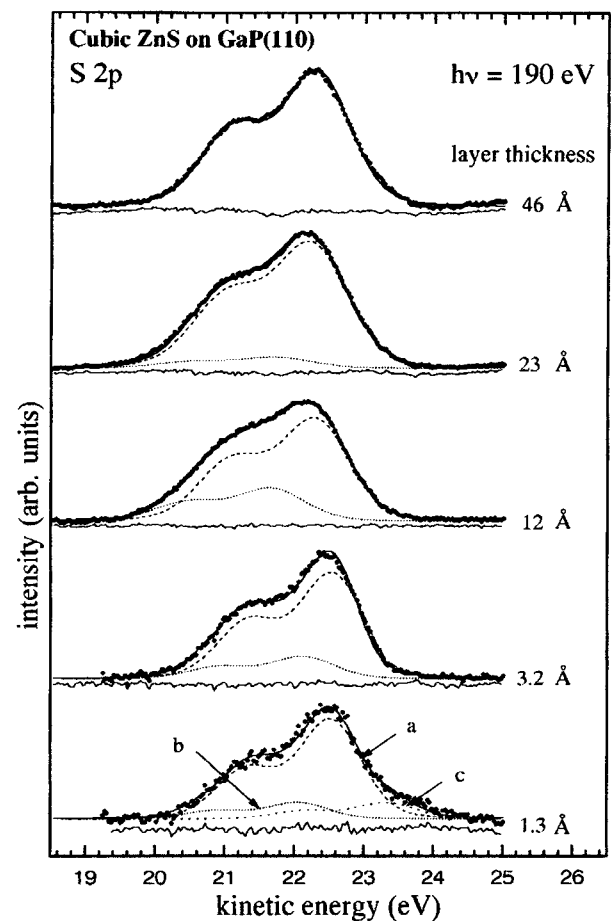


Fig. 3. Selected spectra showing changes in the sulfur 2*p* core level during ZnS growth on GaP(110). The dominant peak (a) is due to Zn–S bonding, and the lower kinetic energy peak (b) indicates Ga–S bonding which results from a coverage-dependent chemical reaction which is confined to the interfacial region.

H₂S. This may be due to the presence of zinc which could contain the phosphorus in the bulk, or the higher growth temperature resulting in phosphorus desorption. A simple interpretation would then be a Zn–Ga exchange, accompanied by Ga–S interface bonding.

In order to further test this simple picture, the emission from the sulfur 2*p* level was also measured as the ZnS layer was grown and selected spectra are shown in Fig. 3. All spectra have been normalized to equal height for clarity, and each spectrum includes the fit components and the total fitted curve. At low coverages, the lower intensity precludes an accurate resolution of the spectra into components, although the coverage of 1.3 Å clearly requires three components (a),(b),(c) as shown. Peak (c) is absent at the next coverage, and subsequent peaks can be fitted using only the two components (a),(b). The origin of peak (c) remains unclear, but this peak is absent above a coverage of 1.3 Å indicating that it is unlikely to be due to gallium–sulfur bonds; it might be due to sulfur–sulfur bonds in the initial stages of growth.

Peak (a) remains dominant throughout and at a coverage of 46 Å no other peak is present. As this corresponds to the

point at which there is no substrate gallium and phosphorus emission, peak (a) is ascribed to sulfur atoms in bulk ZnS. At 23 Å, a second, lower kinetic energy peak is present, although with a low relative intensity. This peak (b) is present, in varying amounts at all lower coverages, with a broadening larger than peak (a). The intensity of this feature relative to the ZnS peak (a) appears to reach a maximum at 12 Å. Since the increase in relative intensity follows the increase in the corresponding low kinetic energy feature in the gallium 3*d* emission, this peak is ascribed to gallium–sulfur bonding at the interface. The intensity change suggests that the extent of intermixing at the interface increases up to a coverage of 12 Å and then ceases. At higher coverages, therefore, peak (b) does not contribute to the sulfur 2*p* signal. [Note that one (110) double layer of ZnS is about 3.82 Å, and so 12 Å corresponds to about three double layers.] Since the intensity of peak (b) never exceeds 30% of the intensity of peak (a), the gallium–sulfur compound formation is confined to the interface region. It is interesting to note that the lattice constant of gallium sesquisulfide Ga₂S₃ [5.44 Å (Ref. 16)] is close to that of both GaP and cubic ZnS, such that the formation of this phase at the interface would not present an obstacle to epitaxial growth of ZnS on GaP, as for other similar heterojunctions.²⁰

The persistence of the peak at 23 Å indicates that the growth is not fully layer by layer, but the film is completely closed at 46 Å. As for the substrate gallium and phosphorus emission peaks, a shift in all peaks to lower kinetic energy at 12 Å reflects the charging of the increasingly insulating layer. The Zn 3*d* band (not shown) also has a low intensity low-energy component at coverages below 3.2 Å, indicating that there is small amount of zinc–substrate bonding in the interfacial region. LEED diffraction patterns such as shown for clean GaP(110) and a ZnS overlayer of 260 Å thickness revealed the pattern expected from the growth of a layer of cubic ZnS, with sharp diffraction spots and a low diffuse background, suggesting overlayer growth of good crystalline quality, but no attempts at a quantification of crystalline quality were made in the present study.

B. Valence levels and heterojunction band offset

Having established the growth of cubic ZnS layers of (110) orientation with good crystalline quality, we proceed to evaluate the valence band spectra in terms of cubic ZnS bulk bands, and to establish the band offsets between GaP(110) and cubic ZnS. The valence band spectrum of GaP(110) covered with different amounts of ZnS is shown as a function of deposition in Fig. 4, recorded at a photon energy of 80 eV. The spectrum is found to shift to higher binding energies, and to gradually change its appearance with deposition; the sharp peak at 2 eV below the VBM is attenuated, and a broader group of peaks appears at 2 eV below the VBM of ZnS (top spectrum). The VBM is shifted by about 0.46 eV with respect to the second GaP spectrum from the bottom; the shift between the first and second spectrum from the bottom is due to band bending as in the Ga 3*d* peak in Fig. 1. The spectra at intermediate coverages can be viewed as a

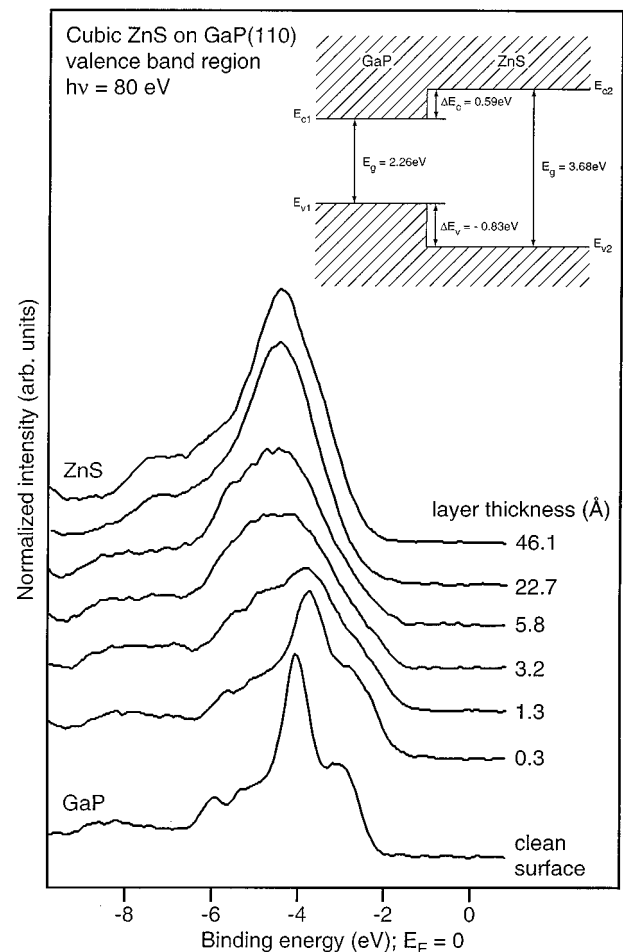


Fig. 4. Valence band spectra of clean GaP(110) (bottom curve) and increasing thicknesses of ZnS as indicated. Note the shift of the valence band maximum to lower kinetic energies as the ZnS layer is built up. Inset: arrangement of valence band maxima, and magnitude of valence and conduction band offsets derived from our experimental results.

superposition of contributions from the top (ZnS) and bottom (GaP) spectra, possibly with some additional contribution from the interface reaction layer, which cannot be resolved here. What is evident from this set of spectra is the shift of the valence band maximum (VBM) towards lower energies, indicative of the formation of a valence band offset ΔE_v . The magnitude of ΔE_v cannot be derived directly from the shift of the VBM itself, since band bending in the substrate occurs upon overlayer deposition, as evidenced through the shift of the GaP-derived valence spectrum. Upon deposition of the first layer, all spectral features shift by 0.46 eV. This shift is identical to that observed on the gallium 3*d* and phosphorus 2*p* peaks, which confirms its origin as being due to band bending. Based on this value for the band bending shift, we evaluate the valence band offset as $\Delta E_v = 0.83$ eV. From the band gap of GaP of 2.26 eV²¹ and that of cubic ZnS of 3.68 eV⁸ this leads to a conduction band offset of 0.59 eV, i.e., the heterojunction is of the straddling type.

Cubic ZnS on GaP is one of the lattice-matched heterojunctions, which are amenable to superlattice calculations of

band offsets such as performed for similar systems (see, for example, Ref. 22). However, for this particular heterojunction such detailed theoretical considerations are not available. An appropriate scheme for this system is then the dielectric midgap energy (DME) model of Cardona and Christensen²³ which bases its predictions of ΔE_V on bulk semiconductor properties. The DME model²³ for ZnS/GaP yields a value for ΔE_V of 1.17 eV, i.e., a discrepancy of 0.34 eV or almost 40% of the entire band offset. Other schemes that rely on bulk properties yield even higher values. On the basis of a recent calculation,²⁴ the bond ionicities of GaP (0.36) and ZnS (0.76) show a large difference as expected. For a similar difference in ionicities (e.g., the ZnSe/GaAs system), a supercell calculation of dipole effects at the interface²⁵ yields a reduction of up to 0.77 eV in the magnitude of the band offset through the influence of the interface dipole. Thus the discrepancy between our present experimental results and the DME predictions is not too disturbing, but a supercell calculation of the present system would be desirable.

IV. CONCLUSION

Epitaxial films of cubic zinc sulfide of good crystalline bulk and surface quality have been grown on GaP(110) by molecular beam epitaxy. The core-level photoelectron spectra show layerwise growth and the presence of a small amount of interface reaction leading to the formation of a Ga-S compound. The valence band offset has been evaluated at 0.83 eV, which shows that this system is of the straddling type, with the offset distributed about equally between the valence and conduction bands.

ACKNOWLEDGMENTS

The authors acknowledge the expert technical support by H. Haak and the help of the staff of the Berliner Speicherring Gesellschaft für Synchrotronstrahlung GmbH (BESSY). The authors thank the EPSRC for providing them with access to the Daresbury Laboratory Synchrotron Radiation Source.

This work was supported through Bundesministerium für Forschung und Technologie under Grant No. 05-5-EBFXB0-5-Tp-02, and through European Community HCM-LSI program Contract No. CHGE-CT93-007.

- ¹J. Ding, H. Jeon, M. Hagerott, A. V. Nurmikko, W. Xie, D. C. Grillo, M. Kobayashi, and R. L. Gunshor, *International Conference on the Physics of Semiconductors* (World Scientific, Beijing, 1992).
- ²R. K. Swank, *Phys. Rev.* **153**, 844 (1967).
- ³R. Z. Bachrach, R. S. Bauer, S. A. Flodström, and J. C. MacMenamin, *Nuovo Cimento B* **39**, 704 (1977).
- ⁴C. B. Duke, A. Paton, and A. Kahn, *J. Vac. Sci. Technol. A* **2**, 515 (1984).
- ⁵L. Ley, R. A. Pollak, F. R. McFeely, S. P. Kowlaczyk, and D. A. Shirley, *Phys. Rev. B* **9**, 600 (1974).
- ⁶J. F. Bernard and A. Zunger, *Phys. Rev. B* **36**, 3199 (1987).
- ⁷V. Fiorentini, M. Methfessel, and M. Scheffler, *Phys. Rev. B* **47**, 13 (1993).
- ⁸Landolt-Börnstein, in *Intrinsic Properties of Group IV and III-V, II-VI and I-VII Compounds*, edited by O. Madelung (Springer, Berlin, 1992).
- ⁹C. Maierhofer, S. Kulkarni, M. Alonso, T. Reich, and K. Horn, *J. Vac. Sci. Technol. B* **9**, 2238 (1991).
- ¹⁰W. G. Wilke and K. Horn, *J. Vac. Sci. Technol. B* **6**, 1211 (1988).
- ¹¹W. G. Wilke, R. Seedorf, and K. Horn, *J. Vac. Sci. Technol. B* **9**, 807 (1989).
- ¹²G. Neuhold, K. Horn, K. O. Magnusson, and D. A. Evans, *J. Vac. Sci. Technol. A* **13**, 666 (1995).
- ¹³A. B. McLean and R. Ludeke, *Phys. Rev. B* **39**, 6223 (1989).
- ¹⁴T. Chasse, M. Alonso, R. Cimino, W. Theis, W. Braun, and K. Horn, *Appl. Surf. Sci.* **64**, 329 (1993).
- ¹⁵A. Krost, W. Richter, and D. R. T. Zahn, *Semicond. Sci. Technol. A* **6**, 109 (1991).
- ¹⁶R. G. Wyckoff, *Crystal Structures* (Interscience, New York, 1963).
- ¹⁷P. Moriarty, B. Murphy, L. Roberts, A. A. Cafolla, G. Hughes, L. Koenders, and P. Bailey, *Phys. Rev. B* **50**, 14237 (1994).
- ¹⁸B. Murphy, P. Moriarty, L. Roberts, A. A. Cafolla, G. Hughes, L. Koenders, and P. Bailey, *Surf. Sci.* **317**, 73 (1994).
- ¹⁹E. Dudzik, C. Muller, I. T. McGovern, D. R. Lloyd, A. Patchett, D. R. T. Zahn, T. Johal, and R. McGrath, *Surf. Sci.* **344**, 1 (1995).
- ²⁰W. G. Wilke, R. Seedorf, and K. Horn, *J. Cryst. Growth* **101**, 620 (1990).
- ²¹Landolt-Börnstein, in *Physics of Group IV Elements and III-V Compounds*, edited by O. Madelung (Springer, Berlin, 1982), Vol. III/17a.
- ²²C. G. V. d. Walle and R. M. Martin, *Phys. Rev. B* **35**, 8154 (1987).
- ²³M. Cardona and N. E. Christensen, *J. Vac. Sci. Technol. B* **6**, 1285 (1988).
- ²⁴N. E. Christensen, S. Satpathy, and Z. Pawlowska, *Phys. Rev. B* **36**, 1032 (1987).
- ²⁵N. E. Christensen, *Phys. Rev. B* **37**, 4528 (1988).